HHS Public Access

Author manuscript

Neurosci Lett. Author manuscript; available in PMC 2017 September 09.

Published in final edited form as:

Neurosci Lett. 2016 November 10; 634: 70–75. doi:10.1016/j.neulet.2016.10.011.

Mechanical sensitivity and electrophysiological properties of acutely dissociated dorsal root ganglion neurons of rats

Viacheslav Viatchenko-Karpinski and **Jianguo G. Gu**

Department of Anesthesiology and Perioperative Medicine, College of Medicine, University of Alabama at Birmingham, 901 19TH Street South, BMR II 210, Birmingham, AL 35294

Abstract

Primary afferent fibers use mechanically activated (MA) currents to transduce innocuous and noxious mechanical stimuli. However, it is largely unknown about the differences in MA currents between the afferents for sensing innocuous and noxious stimuli. In the present study, we used dorsal root ganglion (DRG) neurons acutely dissociated from rats and studied their MA currents and also their intrinsic membrane properties. Recorded from small-sized DRG neurons, we found that most of these neurons were mechanically sensitive (MS) showing MA currents. The MS neurons could be classified into nociceptive-like mechanically sensitive (Noci-MS) and non-nociceptive-like mechanically sensitive (nonNoci-MS) neurons based on their action potential shapes. Noci-MS neurons responded to mechanical stimulation with three types of MA currents, rapidly adapting (RA), intermediately adapting (IA), and slowly adapting (SA) currents. In contrast, almost all nonNoci-MS neurons showed RA current type in response to mechanical stimulation. Mechanical thresholds had a broad range for both nonNoci-MS and Noci-MS neurons, and the thresholds were not significantly different between them. However, MA current densities were significantly smaller in Noci-MS than in nonNoci-MS neurons. Noci-MS and nonNoci-MS neurons also showed significant differences in their electrophysiological properties including action potential (AP) thresholds and AP firing patterns. These differences may contribute to the differential sensory encoding for innocuous and noxious mechanical stimuli.

Keywords

Mechanotransduction; pain; Piezo2; mechanically activated channels; dorsal root ganglion

Introduction

Many primary afferent endings in the skin and other tissues detect mechanical stimuli such as gentle touch, stretch, and noxious pinch. This is important for sensory tasks including social interaction, environment exploration and avoiding harmful stimuli. The first step

Correspondence and requests for the materials should be addressed to: Jianguo G. Gu, M.B., Ph.D. Department of Anesthesiology and Perioperative Medicine, College of Medicine, University of Alabama at Birmingham, 901 19TH Street South, BMR II 210, Birmingham, AL 35294, gujo@uc.edu.

Author Contributions: V.V.K. performed patch-clamp recordings from DRG neurons and data analysis. J.G. designed the study and wrote the manuscript.

COMPETINGNG FINANCNCIAL INTERESTS: The authors declare no competing financial interests.

toward achieving these tasks is mechanotransduction that conveys mechanical stimuli into electrical signals. Mechanotransduction is found to be mainly mediated by mechanically activated (MA) ion channels in primary afferent neurons (1–5), and these ion channels largely contribute to the mechanical sensitivity of primary afferent fibers.

Mechanically sensitive (MS) afferent neurons have been observed in dorsal root ganglion (DRG) neurons in culture, and these neurons respond to membrane displacements with MA currents. MA currents in DRG neurons display a wide range of kinetics from rapidly adapting (RA), intermediately adapting (IA), to slowly adapting (SA) (2,6). RA currents in DRG neurons have decay time constants of less than 10 ms (2,3,6). The molecular identity conferring RA currents in DRG neurons has recently been elucidated to be Piezo2, a large transmembrane protein that forms MA channels in mammalian primary afferent neurons (6). Piezo2 channels are also expressed on Merkel cells of hair follicles and touch domes of the skin, where they are key molecules for the transduction of gentle touch (7–9). The molecular identities mediating IA currents and SA currents in DRG neurons are not fully understood, but a recent study has identified tentonin 3 as an ion channel mediating MA currents with slow kinetics in a subpopulation of DRG neurons with proprioceptive function (10). Although the role of primary afferent Piezo2 channels in gentle touch has recently been demonstrated using conditioning Piezo2 knockout mice, their potential role in mechanical nociception remains to be determined (11).

Most of previous studies have used cultured DRG neurons to study sensory functions of MA channels (1,3,6). It has been shown with cultured DRG neurons that many capsaicin-sensitive neurons responded to mechanical stimulation with MA currents displaying either RA or SA current kinetics (Drew et al. 2002). This finding may suggest a potential role of MA currents in mechanical nociception. However, DRG neurons grown in culture change their functional phenotypes by altering their nociceptive markers, transducer expression, and intrinsic electrophysiological properties. MA currents have also been found to be significantly affected by nerve growth factors that are commonly used for culturing DRG neurons (12). These changes due to culture conditions may have obscured functions of MA channels in terms of their roles in mechanical transduction for non-nociceptive and nociceptive neurons. In the present study, to minimize the potential cell phenotype changes we used neurons acutely dissociated from rat DRGs and characterized their mechanical sensitivity and electrophysiological properties.

Materials and Methods

Sprague Dawley rats aged 5–9 weeks were used. Animal care and use conformed to NIH guidelines for care and use of experimental animals. Experimental protocols were approved by the Institutional Animal Care and Use Committee of the University of Alabama at Birmingham. Acutely dissociated DRG neurons were prepared as described in our previous work (13). In brief, rats were deeply anesthetized with isoflurane and sacrificed by decapitation. Bilateral DRGs were dissected out and incubated with dispase II (5 mg/ml) and type I collagenase (2 mg/ml) in 2 ml bath solution at 35°C for 45 min. The bath solution was the same one used for cell perfusion in electrophysiology experiments (see below). After a rinse, DRGs were triturated to dissociate the neurons in the bath solution, and the

dissociated cells were plated on glass coverslips coated with poly-D-lysine and maintained at room temperature. Whole-cell patch-clamp recordings were performed within 1 to 4 hours after cell plating.

The cells were perfused with normal bath solution flowing at 1 ml/min in a 0.5 ml chamber on the stage of an Olympus IX70 microscope. The bath solution contained (in mM) 150 NaCl, 5 KCl, 2 $MgCl_2$, 2 $CaCl_2$, 10 glucose, and 10 HEPES, pH of 7.4, osmolarity of 320 mosM. The internal solution of electrodes contained (in mM) 135 K-gluconate, 0.5 $CaCl_2$, 2 $MgCl_2$, 5 KCl, 5 EGTA, 10 HEPES, 2 Na_2-ATP, 0.5 Na_2-GTP, pH of 7.2 and osmolarity of 315–325 mOsm. Recording electrode resistance was ~5 MΩ. The junction potential was −15 mV and was adjusted. The series resistance of each recording was below 30 MΩ and was not compensated. Recording signals were amplified with Axopatch 200B (Axon Instruments), filtered at 2 kHz, and sampled at 5 kHz using pCLAMP 10 (Axon Instruments). Unless otherwise indicated, all reagents were purchased from Sigma.

To determine MA currents, DRG neurons were held at −75 mV and mechanical stimulation was applied to DRG cell bodies using a heat-polished glass pipette as a probe (tip diameter approximately 4 μm). The probe was controlled by a piezo-electric device (Physik Instruments, Auburn, MA). The probe was positioned at an angle of 45° to the surface of the dish. The tip of the probe and the recorded cell were visualized as live images on a monitor. The live images were captured continuously through a CCD camera that was connected to the microscope fitted with a 40× objective. The tip of the mechanical probe was positioned so that a 1 μm movement contacted the cell and was considered as a 1-μm membrane displacement. The probe was moved at a speed of 0.5 μm/ms. Unless otherwise indicated, stepwise membrane displacements were produced by the mechanical probe for up to 15 μm in the increment of 1 μm each step and the duration of each step was 500 ms. To determine membrane and AP properties of recorded DRG neurons, under the whole-cell current-clamp mode, step current pulses were injected into cells through patch-clamp electrodes. The step currents were applied from −50 pA to 1500 pA in an increment of 25 pA per step and the duration of each pulse was 1 s. All recordings were performed at the room temperature of 24°C.

Recording data were analyzed using Clampfit 10 software. Data are reported as mean ± SEM. Statistical significance (*$p < 0.05$, **$p < 0.01$, and ***$p < 0.001$) was assessed by two-way ANOVA with post-hoc Fisher's LSD test.

Results

To enhance the stability of acutely dissociated DRG neurons in recording chambers during patch-clamp recordings of mechanically activated (MA) currents, we used a glass pipette tip as an anchor point to restrict cell movement during membrane displacements (Figure 1A). This modification helped improve the reproducibility of MA currents recorded from acutely dissociated DRG neurons. All recorded neurons were small-sized cells with diameters ≤ 35 μm. Membrane displacement could evoke inward MA currents under the voltage-clamp mode (Figure 1B) and action potential firing under the current-clamp mode (Figure 1C). With membrane displacements up to 15 μm, 82% (n = 73) of DRG neurons were

mechanically sensitive (MS) showing MA currents (Figure 1D), and the remaining 18% (n = 16) cells did not show any detectable MA currents and were considered as mechanically insensitive (MI) cells (Figure 1D). Action potential (AP) shapes have been used as indicators of nociceptive-like (Noci) and non-nociceptive-like (nonNoci) DRG neurons, and a Noci neuron usually has a broad AP with a shoulder during repolarization but a nonNoci neuron has a narrow AP without a repolarization shoulder (14). Accordingly, we classified our DRG neurons into nonNoci (Figure 1E) and Noci neurons (Figure 1F). For MI neurons, most (88%, n = 14) of them were Noci neurons and the remaining 12% (n = 2) were nonNoci neurons (Figure 1G). For MS neurons, 78% (n = 57) of them were Noci neurons and 22% (n = 16) were nonNoci neurons (Figure 1H).

MA currents recorded from our acutely dissociated DRG neurons showed a broad range of kinetics from rapidly adapting (RA, Figure 2A), intermediate adapting (IA, Figure 2B), to slowly adapting (SA, Figure 2C). The histogram (n = 73) of MA current decay time constants showed a distribution skewed to the cells with the RA current type (Figure 2D). There was no discretionary subpopulations of MS cells that could be identified from the time constant histogram (Figure 2D). We arbitrarily classified MA currents with τ < 10 ms as RA current, τ = 10 – 50 ms as IA currents, τ > 50 ms as SA currents. Using this classification, most (59%, n = 43) of our MS cells showed RA currents; 30% and 8% of our MS cells displayed IA and SA currents, respectively (Figure 2E). The averaged decay time constants (Figure 2F) for each of the RA, IA, and SA cell categories were 5.85 ± 0.39 ms (n = 43), 17.51±1.6 ms (n = 22), and 96.79±15.14 ms (n = 8), respectively. When these MS cells were sub-classified into nonNoci and Noci neurons, it was found that almost all nonNoci-MS neurons (14/16) displayed RA currents; only 2 cells showed IA currents and no nonNoci MS neurons showed SA currents (Figure 2G). In contrast, In addition to RA currents which were seen in about 51% (29/57) of Noci-MS neurons, IA and SA currents were observed in 25% (14/57) and 14% (8/57) of Noci-MS neurons, respectively (Figure 2G).

Mechanical thresholds, the minimal membrane displacements required to evoke detectable MA currents, exhibited a broad range from 1 to 12 μm (Figure 3A) among all MS DRG neurons recorded (Figure 3A). Threshold histogram for these MS cells shows a normal distribution with most MS cells having their mechanical threshold being 3–5 μm (Figure 3A). There was no indication for the presence of sub-populations of MS cells that had discretionary mechanical threshold based on the histogram (Figure 3A). Separating Noci-MS and nonNoci-MS neurons for the threshold histogram also did not show any segregation in the threshold distribution between these two groups of MS cells (Figure 3B). For Noci-MS cells, threshold distribution of cells with RA, IM and SA currents were further examined and the histogram also did not show differences in threshold distribution among Noci-MS neurons with different types of MA currents (Figure 3C). Averaged thresholds (Figure 3D) for nonNoci-MS (4.13 ± 0.36 μm, n =16), noci-MS (4.86 ± 0.3 μm, n = 57), nonNoci-RA (4.14 ± 0.4 μm, n =14), Noci-RA (4.79 ± 0.43 μm, n =29), Noci-IA (4.8 ± 0.48 μm, n =20), and Noci-SA (5.25 ± 0.84 μm, n =8) were all not significantly different from each other. However, MA current densities were found to be lower in Noci-MS neurons than in nonNoci-MS neurons (Figure E&F) when comparison was made at the same displacements (Figure 3E) or at the same increment of displacement after threshold (Figure 3F). The

statistically significant differences were seen when displacements were ≥ 6 μm (Figure 3E) or displacement of ≥ 4 μm after thresholds (Figure 3F).

MS neurons showed two types of action potential (AP) firing patterns, single AP and multiple APs, in response to step-wise depolarizing currents. Interestingly, Noci-MS and nonNoci-MS neurons showed significant differences in action potential firing patterns. Almost all nonNoci-MS neurons (15/16; 13/14 RA and 2/2 IA cells) exhibited single action potential firing pattern in response to membrane depolarization, and only 1 out of 16 nonNoci-MS neurons showed multiple firing pattern (Figure 4B). In contrast, the majority of Noci-MS neurons (34/57; 19/29 RA, 10/20 IA, and 5/8 SA cells) showed multiple action potential firing pattern, the remaining (23/57) Noci-MS neurons firing only single action potentials in response to membrane depolarization (Figure 4C). We compared other membrane and action potential properties of Noci-MS subgroups (Noci-RA, Noci-IM, Noci-SA) to nonNoci-RA neurons (Table 1). Although all cells in the present study were considered to be small-sized cells with their soma diameters ≤ 35 μm, cell sizes of Noci-MS of each subgroup (Noci-RA/single-AP, Noci-RA/multiple-AP, Noci-IA/single-AP, Noci-IA/multiple-AP, Noci-SA/multiple-AP) were significantly smaller than those of nonNoci-RA cells. Similarly, membrane capacitance of each subgroup of Noci-MS neurons was significantly smaller than that of nonNoci-RA cells. Membrane input resistance of each subgroup of Noci-MS neurons was higher than that of nonNoci-RA cells. AP rheobase of each subgroup of Noci-MS cells was not significantly different from that of nonNoci-RA cells. However, action potential thresholds were in the range of −22 to −30 mV for Noci-MS cell subgroups, and were significantly higher than that of nonNoci-RA cells (−42.5 ± 1.5 mV, n = 13, $P < 0.001$). Finally, action potential widths of Noci-MS subgroups had long duration of 6.2 ± 0.73 to 7.7 ± 1.07 ms, significantly longer than those of nonNoci-RA neurons (1.29 ± 0.13 ms).

Discussion

In the present study we have characterized mechanical sensitivity and electrophysiological properties of small-sized DRG neurons acutely dissociated from rats. We classify these cells into non-nociceptive-like and nociceptive-like neurons based on their action potential shapes (14) although DRG neurons consist of many more functional subgroups. We show that almost all nonNoci-MS cells responded to membrane displacements with RA currents. In contrast, about 51% Noci-MS showed RA currents and the remaining 49% showed either IA currents or SA currents in responses to membrane displacements. The RA currents in DRG neurons have been identified to be mainly mediated by Piezo2 channels (6). Thus, Piezo2 channels may be mechanical transducers for almost all nonNoci-MS neurons but only for about 50% of Noci-MS neurons in our study. The presence of Piezo2 channels in our small-sized nonNoci-MS DRG neurons raises a possibility that these afferents may be c- or Aδ-low threshold mechanoreceptors (LTMR), and some of them may be the c/Aδ-LTMR in the lanceolate endings of hair follicles (15). On the other hand, the presence of Piezo2 channels in our small-sized Noci-MS DRG neurons would suggest that Piezo2 channels could play a role in nociceptive mechanotransduction. However, genetic deletion of Piezo2 channels in mice showed behavioral deficit only to innocuous but not noxious mechanical stimuli (11). The lack of behavioral deficit in the Piezo2 knockout mice could be due to a compensatory

mechanism. This is highly possible since about 50% of Noci-MS neurons transduce mechanical stimuli into IA and SA currents rather than Piezo2-like RA currents in the present study. IA and SA currents in Noci-MS DRG neurons may be mediated by tentonin 3, another recently identified MA channels that display slower kinetics (10), or unidentified MA channels. Some IA and SA currents could also be due to the alteration of Piezo2 channel inactivation kinetics due to osmotic swelling (16).

Innocuous and noxious mechanical stimuli are thought to be transduced by LTMRs and high threshold mechanoreceptors (HTMRs), respective. A previous study using cultured DRG neurons has shown differences in the thresholds of MA currents evoked from different subgroups of DRG neurons (4). However, we did not see any significant differences in the thresholds for evoking MA currents between nonNoci and Noci-MS neurons. There is also no significant difference in the thresholds for evoking RA, IA, and SA currents. The discrepancy between the present study and the previous one could be due to the differences in cell preparation as the previous study used cultured DRG neurons. It also could be because larger cells were included in the previous study but not in the present study. Our results may suggest that functionally defined LTMRs and HTMRs are not necessarily due to their differences in mechanical transduction thresholds. We found that MA current density was significantly lower in Noci-MS neurons than in nonNoci-MS neurons, and this difference could be an important contributing factor for some functionally defined non-nociceptive LTMRs and nociceptive HTMRs.

Noci-MS and nonNoci-MS neurons show significant differences in their intrinsic membrane properties. Almost all nonNoci-MS showed single AP firing pattern while most Noci-MS neurons displayed multiple AP firing patterns. The patterns of AP firing in these MS neurons may be a determinant for functionally defined rapidly adapting or slowly adapting mechanoreceptors. Consistently, slowly adapting responses are commonly seen in nociceptive mechanoreceptors (17). There are other differences in membrane and action potential properties between nonNoci-MS and each subgroup of Noci-MS neurons. Each subgroup of Noci-MS neurons has significantly higher AP threshold than those of nonNoci-MS. A higher AP threshold in Noci-MS would require mechanical stimulation at high intensity to induce sensory impulses in nociceptive mechanoreceptor endings.

Taken together, our study suggests that MA current densities and electrophysiological properties, rather than mechanical thresholds, may be related to mechanical functions of the nonNoci-MS neurons and Noci-MS neurons investigated in the present study. In addition, nociceptive mechanical transduction may be mediated by Piezo2 channels as well as other mechanoreceptors.

Acknowledgments

We thank Dr. Alan Randich for comments on an earlier version of this manuscript. This work was supported by NIH grants DE018661 and DE023090 to J.G.G.

References

1. McCarter GC, Reichling DB, Levine JD. Mechanical transduction by rat dorsal root ganglion neurons in vitro. Neurosci Lett. 1999; 273:179–182. [PubMed: 10515188]

2. Drew LJ, Wood JN, Cesare P. Distinct mechanosensitive properties of capsaicin-sensitive and -insensitive sensory neurons. J Neurosci. 2002; 22:RC228. [PubMed: 12045233]

3. Hu J, Lewin GR. Mechanosensitive currents in the neurites of cultured mouse sensory neurones. J Physiol. 2006; 577:815–828. [PubMed: 17038434]

4. Coste B, Crest M, Delmas P. Pharmacological dissection and distribution of NaN/Nav1.9, T-type Ca2+ currents, and mechanically activated cation currents in different populations of DRG neurons. J Gen Physiol. 2007; 129:57–77. [PubMed: 17190903]

5. Jia Z, Ling J, Gu JG. Temperature dependence of rapidly adapting mechanically activated currents in rat dorsal root ganglion neurons. Neurosci Lett. 2012; 522:79–84. [PubMed: 22743298]

6. Coste B, Mathur J, Schmidt M, Earley TJ, Ranade S, Petrus MJ, Dubin AE, Patapoutian A. Piezo1 and Piezo2 Are Essential Components of Distinct Mechanically Activated Cation Channels. Science. 2010; 330:55–60. [PubMed: 20813920]

7. Ikeda R, Cha M, Ling J, Jia Z, Coyle D, Gu JG. Merkel cells transduce and encode tactile stimuli to drive Abeta-afferent impulses. Cell. 2014; 157:664–675. [PubMed: 24746027]

8. Maksimovic S, Nakatani M, Baba Y, Nelson AM, Marshall KL, Wellnitz SA, Firozi P, Woo SH, Ranade S, Patapoutian A, Lumpkin EA. Epidermal Merkel cells are mechanosensory cells that tune mammalian touch receptors. Nature. 2014

9. Woo SH, Ranade S, Weyer AD, Dubin AE, Baba Y, Qiu Z, Petrus M, Miyamoto T, Reddy K, Lumpkin EA, Stucky CL, Patapoutian A. Piezo2 is required for Merkel-cell mechanotransduction. Nature. 2014

10. Hong GS, Lee B, Wee J, Chun H, Kim H, Jung J, Cha JY, Riew TR, Kim GH, Kim IB, Oh U. Tentonin 3/TMEM150c Confers Distinct Mechanosensitive Currents in Dorsal-Root Ganglion Neurons with Proprioceptive Function. Neuron. 2016; 91:107–118. [PubMed: 27321926]

11. Ranade SS, Woo SH, Dubin AE, Moshourab RA, Wetzel C, Petrus M, Mathur J, Begay V, Coste B, Mainquist J, Wilson AJ, Francisco AG, Reddy K, Qiu Z, Wood JN, Lewin GR, Patapoutian A. Piezo2 is the major transducer of mechanical forces for touch sensation in mice. Nature. 2014; 516:121–125. [PubMed: 25471886]

12. Di Castro A, Drew LJ, Wood JN, Cesare P. Modulation of sensory neuron mechanotransduction by PKC- and nerve growth factor-dependent pathways. Proc Natl Acad Sci U S A. 2006; 103:4699–4704. [PubMed: 16537426]

13. Xing H, Ling J, Chen M, Gu JG. Chemical and cold sensitivity of two distinct populations of TRPM8-expressing somatosensory neurons. J Neurophysiol. 2006; 95:1221–1230. [PubMed: 16424459]

14. Fang X, McMullan S, Lawson SN, Djouhri L. Electrophysiological differences between nociceptive and non-nociceptive dorsal root ganglion neurones in the rat in vivo. J Physiol. 2005; 565:927–943. [PubMed: 15831536]

15. Abraira VE, Ginty DD. The sensory neurons of touch. Neuron. 2013; 79:618–639. [PubMed: 23972592]

16. Jia Z, Ikeda R, Ling J, Viatchenko-Karpinski V, Gu JG. Regulation of Piezo2 Mechanotransduction by Static Plasma Membrane Tension in Primary Afferent Neurons. J Biol Chem. 2016; 291:9087–9104. [PubMed: 26929410]

17. Handwerker HO, Anton F, Reeh PW. Discharge patterns of afferent cutaneous nerve fibers from the rat's tail during prolonged noxious mechanical stimulation. Exp Brain Res. 1987; 65:493–504. [PubMed: 3556477]

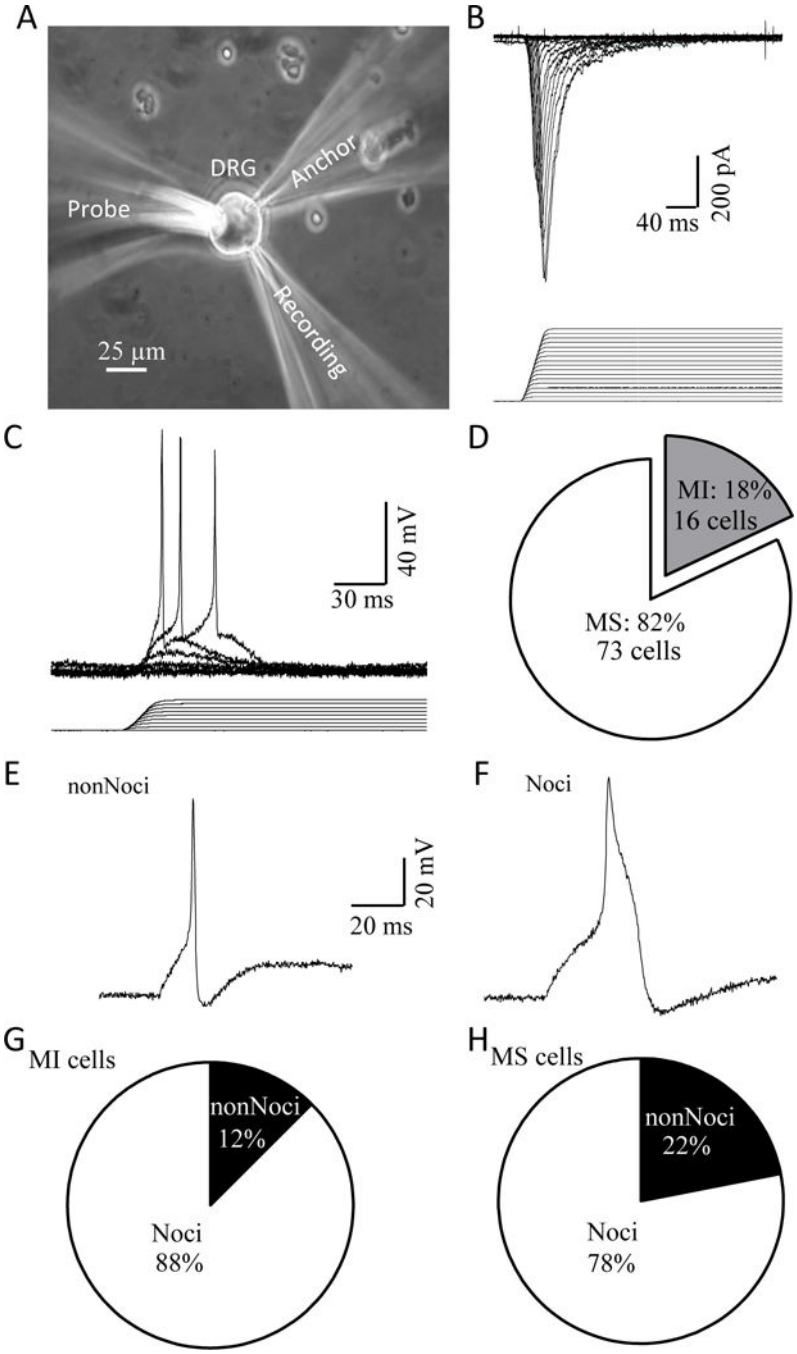

Figure 1. Mechanically activated currents recorded in nociceptive-like and non-nociceptive-like DRG neurons acutely dissociated from rats

A) Experimental setup for patch-clamp recordings of MA currents from acutely dissociated rat DRG neurons. **B**) A set of sample traces of MA currents in a DRG neuron (upper) evoked by stepwise membrane displacements with increment of 1 µm (lower). **C**) Example of mechanically evoked membrane depolarization and action potential firing in a DRG neuron. **D**) Graph shows the fractions of DRG neurons that are mechanically sensitive (MS) showing MA currents (white, 73/89) and mechanically insensitive (MI, 16/89). **E**) An

example of the action potential shape of a non-nociceptive-like (nonNoci) MS DRG neuron. **F**) An example of the action potential shape of a nociceptive-like (Noci) MS DRG neuron. **G**) Fractions of MI neurons that are nonNoci (2/16) and Noci neurons (14/16). **H**) Fractions of MS neurons that are nonNoci 16/73) and Noci (57/73) neurons.

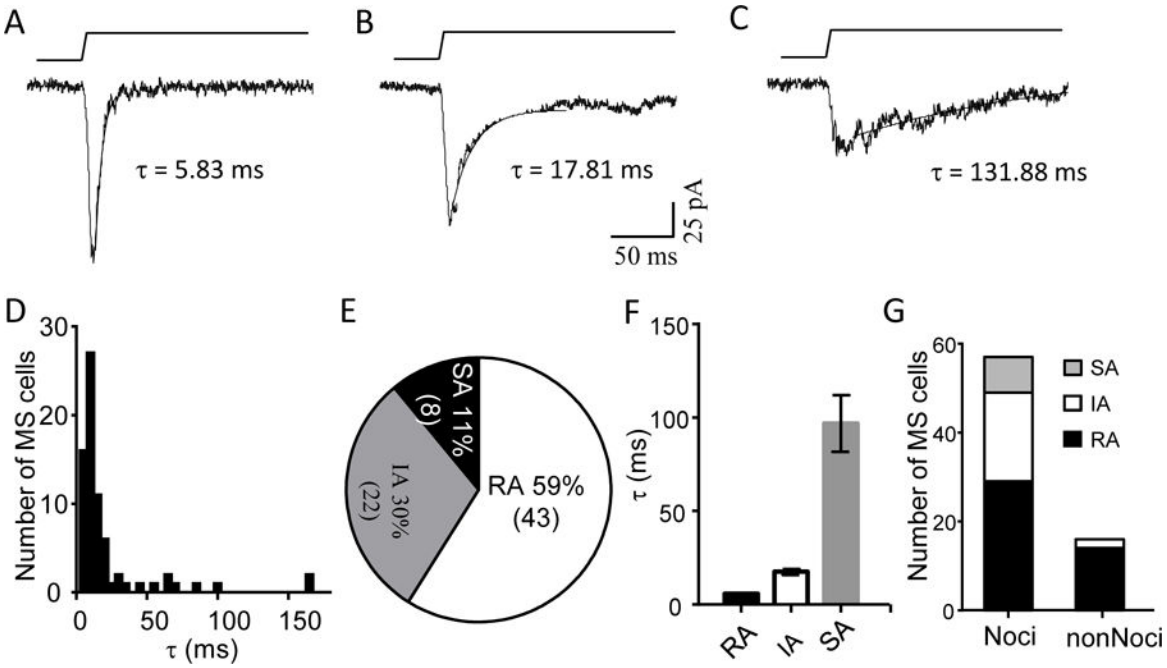

Figure 2. Kinetics of mechanically activated currents in acutely dissociated DRG neurons

A–C) Three sample traces illustrate MA currents that exhibit different kinetics from rapidly adapting (RA, Figure 2A), intermediately adapting (IA, Figure 2B) to slowly adapting (SA, Figure 2C). Decay time constant **τ** of the MA current is show in each figure. Membrane displacement was 7 μm in each test. **D**) Histogram of MS cells with different decay time constants (n = 73). **E**) Graph shows fractions of MS cells with RA (**τ** < 10 ms), IA (**τ** = 10 – 50 ms), or SA (**τ** > 50 ms). **F**) Averaged values of decay time constants of RA (n = 43), IA (n = 22) and SA (n = 8). **G**) Fractions of Noci-MS cells and nonNoci-MS that show MA currents of RA (black), IA (white), SA (gray).

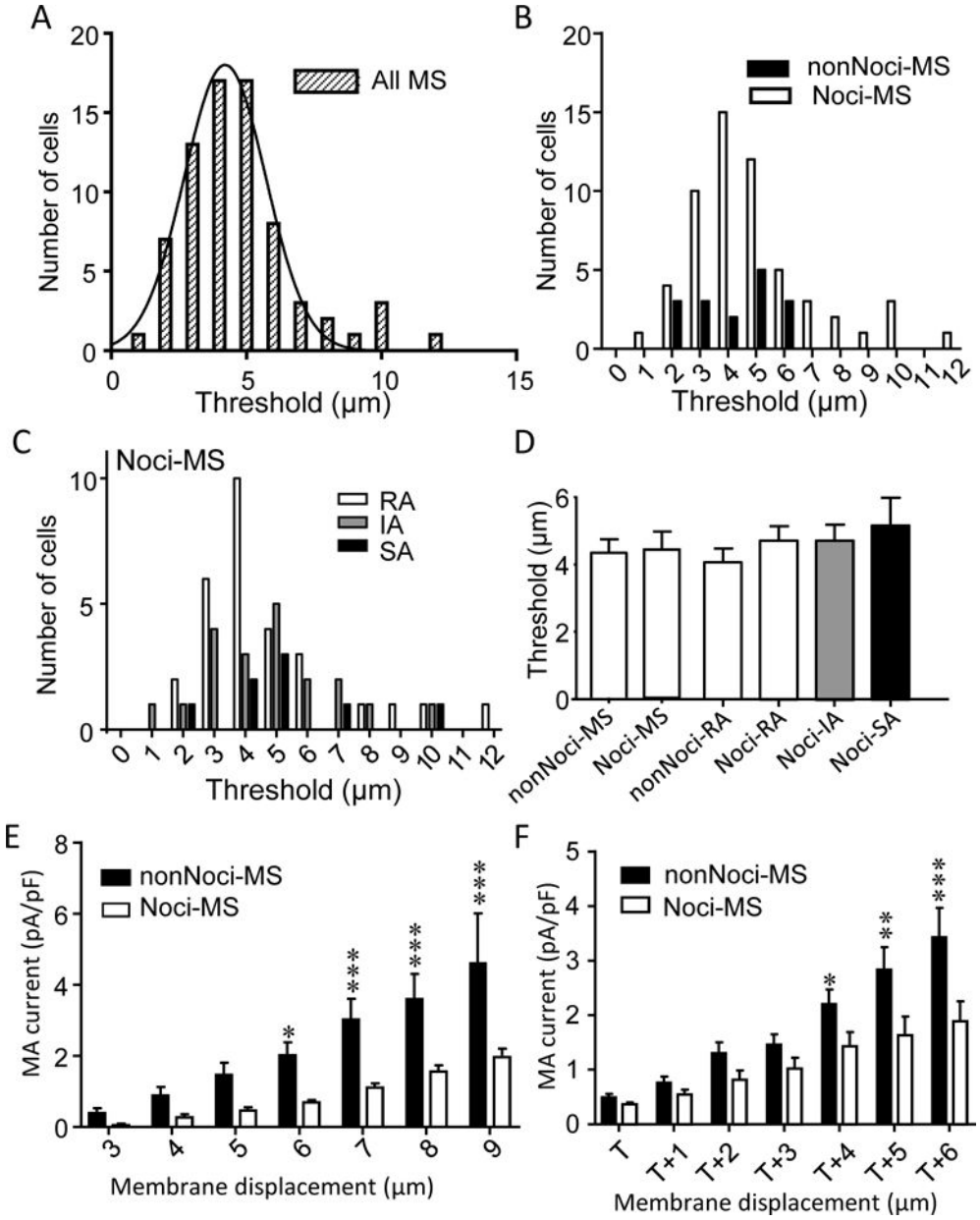

Figure 3. Threshold and density of MA currents in nociceptive-like and non-nociceptive-like DRG neurons

A) Histogram of the thresholds of MS neurons (total 72 cells). **B**) Similar to **A** except MS neurons are divided into nociceptive-like (Noci, n = 56) and non-nociceptive-like (nonNoci, n =16) groups. **C**) Histogram of the thresholds of Noci-MS neuron subgroups of cells with RA (white, n=29), IA (gray, n=20) and SA groups (black, n = 8). **D**) Averaged thresholds of MA currents for nonNoci-MS cells (all kinetic types, n = 16), Noci-MS cells (all kinetic types, n = 57), nonNoci-RA cells (n = 14), Noci-RA cells (n = 29), Noci-IA cells (n = 20), Noci-SA cells (n = 8). **E**) Comparison of MA current density of nonNoci-MS (n = 7) and Noci-MS cells (n = 7) at different membrane displacements. **F**) Comparison of MA current density of nonNoci-MS and Noci-MS cells with displacements scaled to the threshold (T) of

each cell. Data represent Mean ± SEM, *P < 0.05, **P < 0.01, and ***P < 0.001, two-way ANOVA.

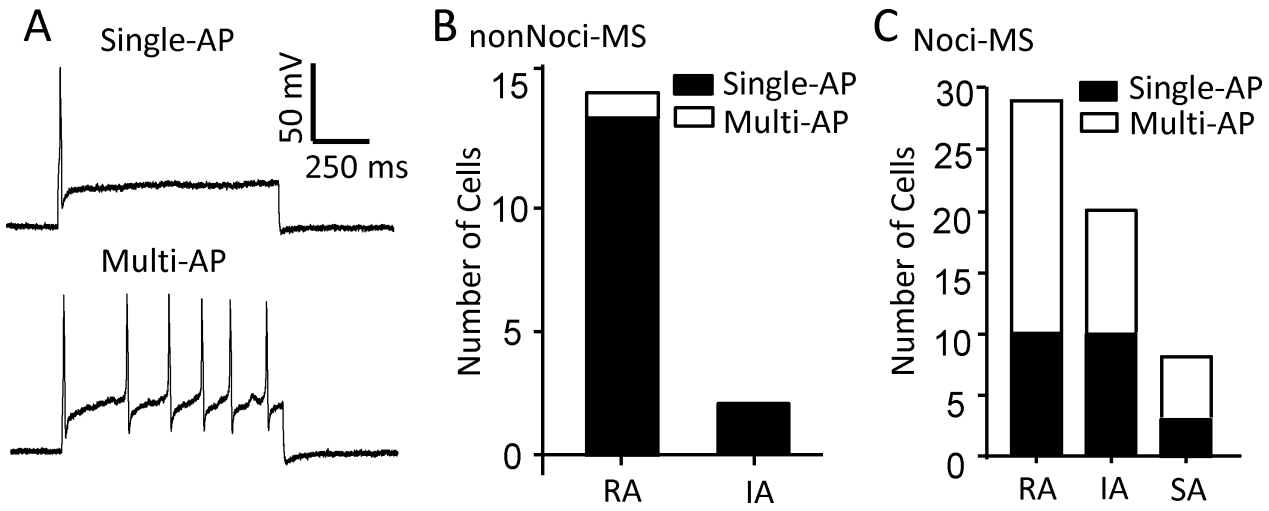

Figure 4. Action potential firing patterns of nociceptive-like and non-nociceptive-like mechanically sensitive DRG neurons

A) Commonly observed action potential firing patterns in nonNoci-MS (single AP, top panel) and Noci-MS (multiple APs, bottom panel). **B**) Numbers of nonNoci-MS cells (nonNoci-RA and nonNoci-IA) showing single AP (black) and multiple APs (white). **C**) Numbers of Noci-MS cells (Noci-RA, Noci-IA and Noci-SA) showing single AP (black) and multiple APs (white).

Table 1

Membrane and AP properties of Noci-MS and nonNoci MS DRG neurons

	Soma diameter (μm)	Membrane capacitance (pS)	Input resistance (MΩ)	AP threshold (mV)	AP rheobase (pA)	AP duration (ms)
nonNoci-RA (n=13)	32.8 ±0.3	42.1 ±2.0	0.20 ±0.02	−42.5 ±1.2	223.1 ±41.4	1.3 ±0.1
Noci-RA, single AP (n=10)	26.7 ±0.6 ***	24.8 ±1.3 ***	0.72 ±0.12 ***	−25.4 ±1.1 ***	292.5 ±50.0	6.5 ±0.9 ***
Noci-RA, multiple AP (n=19)	26.7 ±0.6 ***	20.4 ±1.5 ***	0.81 ±0.09 ***	−24.3 ±1.1 ***	159.2 ±2.9	6.9 ±0.5 ***
Noci-IA, single AP (n=10)	26.5 ±1.0 ***	23.9 ±2.7 ***	0.44 ±0.09 (p = 0.07)	−29.8 ±2.3 ***	217.5 ±41. 7	6.4 ±1.0 ***
Noci-IA, multiple AP (n= 10)	26.3 ±0.8 ***	19.8 ±0.8 ***	0.66 ±0.05 **	−22.2 ±1.5 ***	142.5 ±11.8	7.1 ±1.1 ***
Noci-SA, single AP (n=3)	25.0 ±1.0 NA	24.8 ±2.5 NA	0.77 ±0.37 NA	−21.7 ±1.9NA	150.0 ±76.4 NA	7.7 ±0.9 NA
Noci-SA, multiple AP (n=5)	26.2 ±1.5 ***	23.4 ±3.2 ***	0.85 ±0.16 ***	−29.6 ±4.0 ***	105.0 ±26.7	6.2 ±0.7 **

AP, action potential; Noci, nociceptive; nonNoci, non-nociceptive; RA, rapidly adapting; IA, intermediate adapting; SA, slowly adapting. Data represent mean ± SEM,

** P < 0.01;

*** P < 0.001; NA, not analyzed due to the small sample sizes.